

A Sperm-Associated WD Repeat Protein Orthologous to *Chlamydomonas* PF20 Associates with Spag6, the Mammalian Orthologue of *Chlamydomonas* PF16

Zhibing Zhang,¹ Rossana Sapiro,¹ David Kapfhamer,² Maja Bucan,² Jeff Bray,¹
Vargheese Chennathukuzhi,¹ Peter McNamara,³ Anne Curtis,³ Mei Zhang,⁴
E. Joan Blanchette-Mackie,⁴ and Jerome F. Strauss III^{1*}

Center for Research on Reproduction and Women's Health,¹ Department of Psychiatry,² and Center for Experimental Therapeutics,³ University of Pennsylvania Medical Center, Philadelphia, Pennsylvania 19104, and Lipid Cell Biology Section, Laboratory of Cell Biochemistry and Biology, National Institute of Diabetes and Digestive and Kidney Diseases, National Institutes of Health, Bethesda, Maryland 20892⁴

Received 30 May 2002/Returned for modification 22 July 2002/Accepted 12 August 2002

cDNAs were cloned for the murine and human orthologues of *Chlamydomonas* PF20, a component of the alga axoneme central apparatus that is required for flagellar motility. The mammalian genes encode transcripts of 1.4 and 2.5 kb that are highly expressed in testis. The two transcripts appear to arise from alternative transcription start sites. The murine *Pf20* gene was mapped to chromosome 1, syntenic with the location of the human gene on chromosome 2. An antibody generated against an N-terminal sequence of mouse Pf20 recognized a 71-kDa protein in sperm and testis extracts. Immunocytochemistry localized Pf20 to the tails of permeabilized sperm; electron microscope immunocytochemistry showed that Pf20 was located in the axoneme central apparatus. A murine Pf20-green fluorescent protein fusion protein expressed in Chinese hamster ovary cells accumulated in the cytoplasm. When coexpressed with Spag6, the mammalian orthologue of *Chlamydomonas* PF16, Pf20 was colocalized with Spag6 on polymerized microtubules. Yeast two-hybrid assays demonstrated interaction of the Pf20 WD repeats with Spag6. Pf20 was markedly reduced in sperm collected from mice lacking Spag6, which are infertile due to a motility defect. Our observations provide the first evidence for an association between mammalian orthologues of two *Chlamydomonas* proteins known to be critical for axoneme structure and function.

The “9 + 2” microtubule architecture of the eukaryote axoneme has remained virtually unchanged over millions of years of evolution. Understanding the function of molecules that make up the axoneme is important for elucidating the assembly and activity of these structures that are essential for cell motility. The distinctive arrangement of nine outer doublet microtubules in a circle around a central pair of microtubules is recognizable in electron micrographs of flagella and cilia from plants, algae, protists, and animals. Attached along specific microtubules at precise locations and intervals are ranks of substructures including dynein arms, radial spokes, and central pair projections (25, 26). Axonemal dyneins form the inner and outer arm structures that have different functions; the outer arms add power and adjust beat frequency (3, 4, 10, 15, 16, 24, 33); the inner arms generate the axonemal waveform (4, 7, 14, 17, 27). To work together efficiently, the multiple dynein isoforms must be locally activated and inactivated at different points in the beat cycle, both around the axoneme and along its length.

Structural and genetic evidence implicated the radial spoke-central pair structures as key regulators of dynein activity. The radial spoke heads make transient contact with structures that

project from the central pair microtubules (35). The central pair is composed of two microtubules (designated C1 and C2 in algae) and their associated structures which include the central pair projections, central pair bridges linking the two tubules, and central pair caps which are attached to the distal or plus ends of the microtubules.

Mutants of the alga *Chlamydomonas reinhardtii*, a well-studied model system of ciliary and flagellar function, highlight the importance of the central apparatus. Mutants that lack the central apparatus or some of its components have paralyzed flagella (1, 6, 11, 23, 36). Polypeptide mapping of the *Chlamydomonas* central pair suggests the presence of at least 23 different proteins in addition to tubulin (1, 31). Some of these proteins are uniquely associated with either the C1 or C2 microtubule, indicating that the two microtubules may be functionally specialized. PF16 is located along C1; PF20 is located along the C2 microtubules. To date, the genes encoding four components of the central pair, PF15, PF16, PF20, and KLP1, have been cloned (31). The *Chlamydomonas* PF20 mutant has paralyzed flagella, and isolated axonemes lack the entire central apparatus. The *Chlamydomonas* PF20 gene encodes a 606-amino-acid protein that contains five contiguous WD repeats. These repeats are found in a number of proteins with diverse cellular functions including β -transducin and dynein intermediate chains. Immunogold labeling of wild-type axonemes indicated that PF20 is localized along the length of the C2 microtubule on the intermicrotubule bridges connecting the two

* Corresponding author. Mailing address: Center for Research on Reproduction and Women's Health, 1354 BRB II/III, 421 Curie Blvd., Philadelphia, PA 19104. Phone: (215) 898-0147. Fax: (215) 573-5408. E-mail: jfs3@mail.med.upenn.edu.



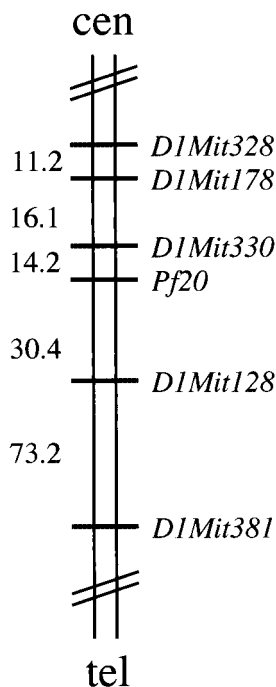


FIG. 2. Map of mouse chromosome 1 and localization of *Pf20*. The *Pf20* gene was placed between markers D1Mit330 and D1Mit128 and is most closely linked to D1Mit330 (log of the odds score of >14). Centiray distances between loci are indicated, 1 cR being equal to 83.7 kb for chromosome 1 (34). cen, centromere; tel, telomere.

central microtubules (32). We have cloned mammalian orthologues of PF20 in order to study the role of central pair proteins in mammalian axoneme assembly and function. Here we describe the interaction of *Pf20* with Spag6, the mammalian orthologue of *Chlamydomonas* PF16, another central apparatus protein containing protein-protein interaction domains (armadillo repeats) that is essential for the structural integrity and function of the axoneme. This information provides a framework for understanding the functionally significant network of interacting proteins in flagella and cilia.

MATERIALS AND METHODS

Animals. Male CD-1 mice were employed for the preparation of protein extracts and RNA. Spag6-deficient mice were generated as previously described (28).

Cloning of the human PF20 and mouse Pf20 cDNAs. A search of public databases identified a human expressed sequence tag (AA832473) which showed high homology to *Chlamydomonas* PF20. Primers were designed to amplify the expressed sequence tag sequence, and the radiolabeled PCR product was used to screen a mouse germ cell cDNA library (Stratagene, La Jolla, Calif.). The inserts of the positive clones were amplified with T₃ and T₇ primers, cloned into pCR 2.1-TOPO TA vector (Invitrogen, Carlsbad, Calif.), and sequenced with an ABI 373A automated sequencer. After the mouse *Pf20* cDNA was cloned, it was used to rescreen a human testis cDNA library (5, 20) with the same protocol used to clone the mouse *Pf20* cDNA.

5' RACE. To obtain the sequence of the 5' end of the mouse *Pf20* cDNA, 5' rapid amplification of cDNA ends (5'-RACE) was performed on mouse testis poly(A)⁺ RNA with the Marathon cDNA amplification kit (Clontech, Palo Alto, Calif.). A primer was designed within the 5' end of the cDNA clone isolated from the mouse germ cell library (5'-AGAAGCCACGAAGTCACCACAGGAGT-3') which was used with the Marathon cDNA adaptor primer to generate 5'-

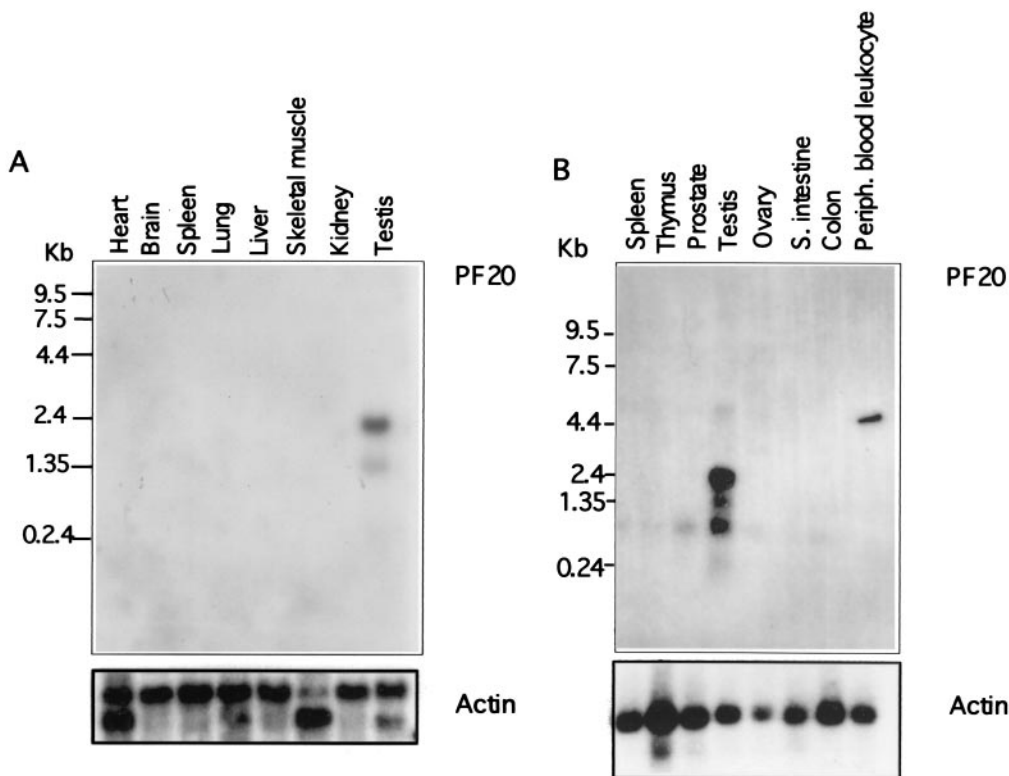


FIG. 3. Northern blot analysis of PF20 mRNAs extracted from indicated tissues. The blots were reprobbed with actin cDNAs. (A) Northern blot analysis of mouse *Pf20* mRNA expression. (B) Northern blot analysis of human *Pf20* mRNA expression. S. intestine, small intestine; Periph., peripheral.

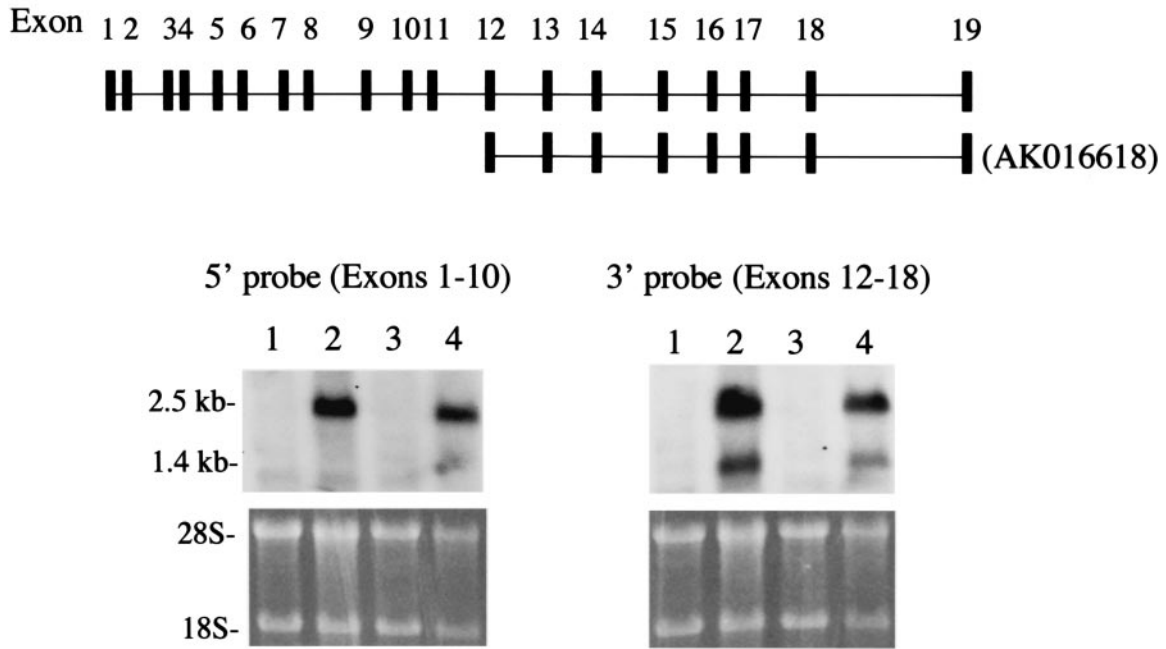


FIG. 4. Deduced genomic structure of the *Pf20* gene and analysis of the two *Pf20* transcripts with region-specific probes. The top shows the deduced genomic structure of the *Pf20* gene and exons included in the 2.5- and 1.4-kb transcripts. Also shown are results of Northern blot analysis with a 5' probe and a 3' probe. Lanes 1 and 3, liver RNA; lanes 2 and 4, testis RNA.

RACE products. The PCR products were cloned into the pCR 2.1-TOPO TA vector and subjected to DNA sequence analysis.

Northern blot analysis. Human and mouse multiple tissue RNA blots were purchased from Clontech. Germ cells were separated by the Staput method (37). Examination of the isolated fractions under Nomarski optics revealed that the purities of the pachytene spermatocytes, round spermatids, and condensing spermatids were 85, 90, and 95%, respectively. Total RNA was isolated with Trizol (Life Technologies, Inc., Grand Island, N.Y.), and 30 μ g of total RNA was separated on a denaturing gel, transferred to a nylon membrane, and hybridized as described previously (28). To characterize the two *Pf20* transcripts, two probes were generated by PCR. The 5' probe encompassing nucleotides coding for

amino acids 20 to 292 was generated with the following primers: forward, 5'-CATTGGCTTGTCCACCCACCG-3', and reverse, 5'-CTCACAACTGTGACCA GC-3'. The 3' probe, encompassing nucleotides coding for amino acid residues 372 to 608, was generated with a forward primer, 5'-CAGATCCAAACGTGAC TTCA-3', and a reverse primer, 5'-CCAGTTTGTGAATTTGCCCGA-3'.

Fusion protein expression and antibody production. A cDNA encoding an N-terminal portion of mouse *Pf20* (amino acid residues 1 to 212) was amplified from a *Pf20* cDNA clone with the following primers: forward, 5'-GGGAATTC CATATGATGGCTGCTCCGTCTGGGGTC-3', and reverse, 5'-CTGAAGCT TCCCCTTTGAGGTCAGCAATGAG-3'. The cDNA was inserted into *Nde*I/*Hind*III sites of the pET28a vector (Novagen, Madison, Wis.). The resulting

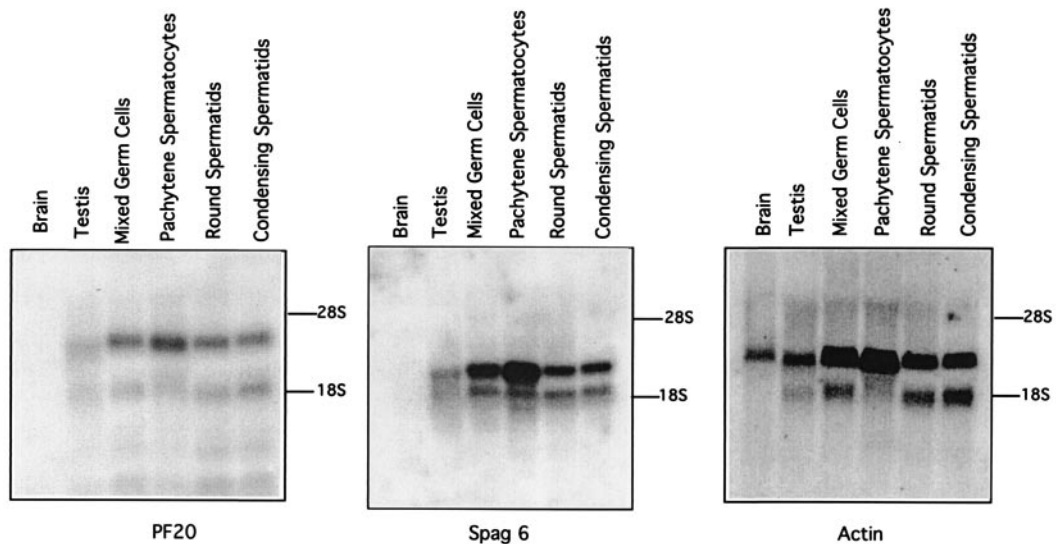


FIG. 5. Expression of *Pf20*, *Spag6*, and actin mRNAs in mouse male germ cells. Northern blots probed sequentially with the indicated cDNAs are shown.

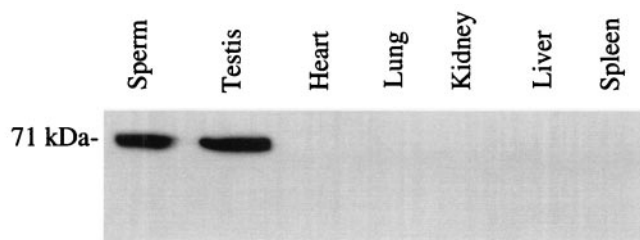


FIG. 6. Western blot analysis of Pf20 protein expression in mouse tissues. The figure shows a Western blot of sperm and tissue protein extracts probed with an antibody generated against the N terminus of the Pf20 protein. An immunoreactive protein band migrating near 71 kDa, compatible with the predicted size of Pf20, is indicated.

fusion protein contains six-His tags at both the NH₂ and C termini. The construct was transformed into BL21(DE3) cells, and fusion protein synthesis was induced with 1 mM isopropyl- β -D-thiogalactopyranoside (IPTG). The cell pellets were sonicated in lysis buffer (100 mM NaH₂PO₄, 10 mM Tris-Cl, 8 M urea, pH 8.0). Bacterial lysates were centrifuged at 13,000 \times g for 30 min and incubated with nitrilotriacetic acid-chelate resin (Qiagen, Valencia, Calif.) at 4°C overnight. The resin was washed with wash buffer (the same as lysis buffer except that the pH was adjusted to 6.3), and the His-tagged protein was eluted with elution buffer (the same as lysis buffer except that the pH was adjusted to 4.5). Eluate fractions were analyzed by sodium dodecyl sulfate-polyacrylamide gel electrophoresis in 10% polyacrylamide gels stained with Coomassie blue. The protein concentration was determined with Pierce reagents (Pierce, Rockford, Ill.). The purified protein was identified on Western blots with an anti-His-tag monoclonal antibody (Novagen). Four injections of 500 μ g of pure protein were used to generate rabbit polyclonal antibody (Rockland, Gilbertsville, Pa.).

Western blot analysis. Equal amounts of protein (50 μ g/lane, except for the sperm, at 10 μ g/lane) were heated to 95°C for 10 min in sample buffer, loaded onto 10% sodium dodecyl sulfate-polyacrylamide gels, electrophoretically separated, and transferred overnight to polyvinylidene difluoride membranes (Millipore Corporation, Bedford, Mass.). Membranes were blocked (Tris-buffered saline solution containing 5% nonfat dry milk and 0.05% Tween 20 [TBST]) and then incubated with the anti-mouse Pf20 antibody (1:600 dilution) at 4°C overnight. After being washed in TBST, the blots were incubated with an anti-rabbit immunoglobulin conjugated to horseradish peroxidase (1:2,000 dilution) for 1 h at room temperature. After washing, the Pf20 protein was detected with Super Signal chemiluminescent substrate (Pierce).

Preparation of sperm for immunolocalization of Pf20. Sperm were obtained from mouse cauda epididymis and centrifuged at 3,000 \times g, washed twice in phosphate-buffered saline (PBS), resuspended in PBS, and layered onto polylysine-coated slides. The preparations were fixed with 4% paraformaldehyde and permeabilized with 1% Triton X-100. Following permeabilization, slides were blocked in PBS containing 10% goat serum (1 h at 37°C) and incubated with primary antibody (rabbit anti-Pf20) overnight at 4°C. The secondary antibody, fluorescein-conjugated goat anti-rabbit immunoglobulin G, was applied, and Pf20 staining was visualized by using an Olympus (Tokyo, Japan) IX-70 epifluorescence microscope and Meta Morph Imaging System software (Universal Imaging Corp., West Chester, Pa.).

Electron microscope immunocytochemistry. Cauda epididymal sperm were fixed and prepared for immunoelectron microscopy as previously described (28). Sections were reacted with anti-mouse Pf20 antibody, washed, and then incubated with rabbit anti-mouse immunoglobulin G labeled with 20-nm gold particles.

Pf20-green fluorescent protein (Pf20-GFP) and Spag6-red fluorescent protein (Spag6-RFP) fusion constructs. A cDNA containing the full coding sequence of mouse Pf20 cDNA was cloned into *EcoRI/BamHI* sites of the pEGFP-N₂ vector, creating the pEGFP/Pf20 plasmid. The Pf20 cDNA was generated with the following primers: forward, 5'-CGAGAATTCTGATGGCTGCTCCGTCTGGGGTC-3', and reverse, 5'-CGCGGATCCCGATCCACAACCGAATGGTGC C-3'. The DNA sequences were confirmed. A murine Spag6-RFP construct was constructed in the pDsRed/N₁ vector.

Cell culture and transient transfection. Chinese hamster ovary cells were obtained from the American Type Culture Collection (Manassas, Va.) and cultured in Dulbecco's modified Eagle's medium containing 10% heat-inactivated fetal bovine serum at 37°C. At 60% confluence, cells were washed twice with serum-free medium before addition of 1 μ g of cDNA encoding the Pf20-GFP

and/or Spag6-RFP fusion proteins and 3 μ l of FuGENE6 (Roche, Indianapolis, Ind.).

Living cells were imaged at room temperature 48 to 72 h after transfection. Confocal images were collected with an LSM410 confocal microscope system equipped with a krypton-argon Omnichrome laser (Carl Zeiss Inc., Thornwood, N.Y.) and a C-Apochromat 63- by 1.2-numerical-aperture water-immersion objective (Zeiss). Excitation wavelengths were 488 nm for GFP and 568 nm for RFP and 488 and 568 nm for dual imaging. Emissions were collected with a 514- to 540-nm band-pass filter for enhanced GFP (EGFP), and a 590-nm long-pass filter for RFP. Adobe Photoshop 5.0 was also used for image processing (Adobe Systems Inc., San Jose, Calif.).

Yeast two-hybrid assays. A cDNA encoding WD repeats of mouse Pf20, which corresponds to amino acids 398 to 639, was subcloned into the *EcoRI/SalI* sites of pBD-GAL4cam (Stratagene) and was used to screen a testis library. The complete coding sequence of Spag6 was subcloned into the *EcoRI/SalI* sites of pAD-GAL4 (Stratagene). The BD-TB-RBP and AD-TB-RBP plasmid constructs used were previously described and contain the complete coding sequence of TB-RBP (2, 5, 37); the AD-TB-RBP₂₀₅ plasmid construct was previously described and contains a cDNA truncated at amino acid 205 of TB-RBP (5, 37). Pairs of BD and AD plasmids were cotransformed into YRG-2, and transformants were selected on synthetic minimal (SD) medium lacking leucine and tryptophan. Protein-protein interactions were detected by growth on SD medium lacking leucine, tryptophan, and histidine. Transformations were performed according to the manufacturer's instructions (Stratagene).

Mapping of the Pf20 gene with a radiation hybrid panel. The mouse *Pf20* gene was mapped with the mouse-hamster T31 radiation hybrid panel previously described (34) and obtained from Research Genetics (Huntsville, Ala.). Briefly, DNA from 100 hybrid lines was used as a template for PCR amplification with a mouse-specific fragment of 130 bp with primers designed from the 3' end of the Pf20 cDNA. Primer sequences and PCR conditions were as follows. The forward primer was 5'-AGGGCATTCCCTCTAAGGCT-3', and the reverse primer was 5'-TGGTCCATATATTATTCACCCAAA-3'. Each PCR mixture contained 25 ng of genomic DNA, 0.23 mM primers, 0.23 mM (each) deoxynucleoside triphosphates, 0.25 U of *Taq* polymerase, and buffer containing 1.5 mM MgCl₂ in a 15- μ l total volume. Thermal cycling consisted of a 5-min denaturation step at 94°C, followed by 35 cycles of 30 s at 94°C, 30 s at 58°C, and 60 s at 72°C and a final 10-min extension at 72°C. PCR products were electrophoresed in 2% agarose gels (Gibco BRL, Grand Island, N.Y.) containing 0.1-mg/ml ethidium bromide solution (Sigma, St. Louis, Mo.).

Nucleotide sequence accession number. The nucleotide sequences of the mouse and human cDNAs and their deduced amino acid sequences have been deposited in GenBank (accession no. AF490390 [mouse] and AF490391 [human]).

RESULTS

Characterization of the human and mouse PF20 cDNAs and their deduced amino acid sequences. Conceptual translation of the cDNA sequences yielded open reading frames of 639 and 631 amino acids for the mouse and human cDNAs, respectively. A unique feature of the encoded polypeptides is contiguous WD (Trp-Asp) repeats in the carboxyl-terminal half of the proteins. The deduced amino acid sequence of the mouse protein was analyzed with the Simple Modular Architecture Research Tool (SMART) program, which revealed a coiled-coil region followed by up to seven contiguous WD repeats. The mouse and human proteins had remarkable amino acid sequence identity-similarity (39% identity for mouse and 44% identity for human; 52% similarity for mouse and 57% similarity for human) to the product of the *Chlamydomonas PF20* gene (Fig. 1). Based on genomic sequences deposited in the GenBank and Celera databases, we deduced that the murine *Pf20* gene consists of 19 exons (see below).

Mapping of the mouse Pf20 gene. To determine the chromosomal location of the mouse *Pf20* gene, the results of our analysis of radiation hybrids were submitted to http://www.genome.wi.mit.edu/cgi-bin/mouse_rh/rhmap-auto/rhmapper.cgi (34), which determines linkage relative to a framework

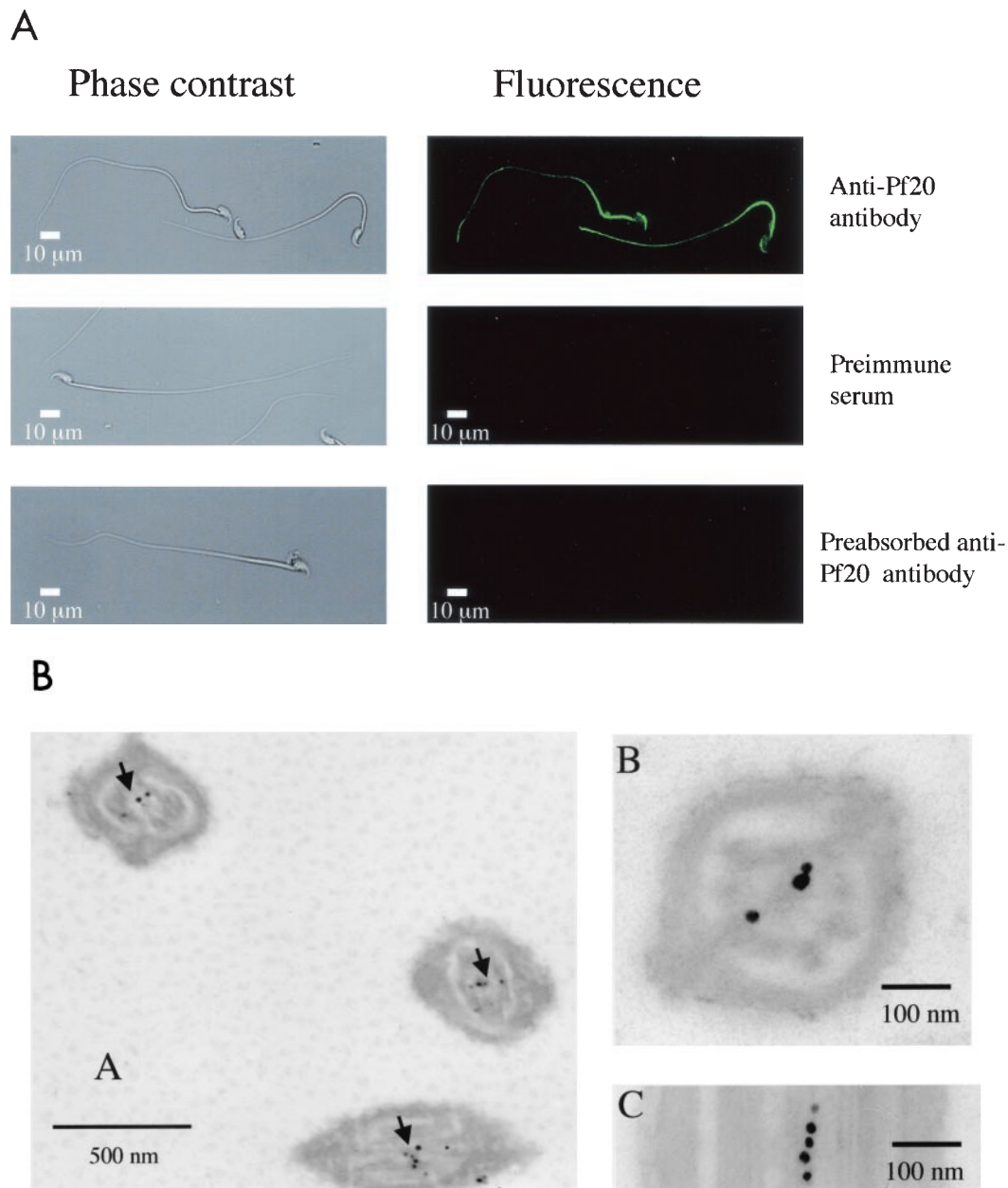


FIG. 7. (A) Localization of Pf20 in mouse sperm flagella. Shown are phase-contrast (left panels) and immunofluorescence (right panels) micrographs of 1% Triton X-100-permeabilized sperm incubated with the anti-Pf20 antibody, preimmune serum, or antibody preabsorbed with recombinant Pf20 antigen. (B) Electron microscopic immunocytochemistry. (Subpanel A) Clustering of gold-labeled antibody in the axoneme cores (arrows). (Subpanel B) Transverse section of a sperm tail showing colloidal gold labeling around the central pair. (Subpanel C) Longitudinal section showing colloidal gold labeling along a central pair microtubule.

map of 2,114 simple sequence length polymorphism (SSLP) markers. The most recent release (http://www-genome.wi.mit.edu/mouse_rh/index.html) reports placement of an additional 8,784 loci on the T31 radiation hybrid panel for a total of 10,898 markers. *Pf20* was most closely linked to framework marker D1Mit330 in the proximal portion of chromosome 1 with a log of the odds (LOD) score of >14 (Fig. 2). This location was subsequently confirmed by a search of the Celera mouse genomic DNA sequence database. A BLAST search of the human PF20 cDNA sequence (<http://genome.ucsc.edu>

[/goldenPath/hgTracks.html](http://goldenPath/hgTracks.html)) confirmed localization of the human gene to 2q34, a region syntenic with mouse chromosome 1. One additional gene, *Bard1* (BRCA1-associated RING domain protein), has been localized between D1Mit330 and D1Mit128 by using the T31 radiation hybrid panel (http://www-genome.wi.mit.edu/mouse_rh/index.html) and maps to 2q34-35 in humans (human draft sequence: <http://www.ncbi.nlm.nih.gov/entrez/viewer.cgi?val=13636653>).

Tissue-specific expression of Pf20. Northern hybridization studies revealed transcripts of 1.4 and 2.5 kb in mouse and

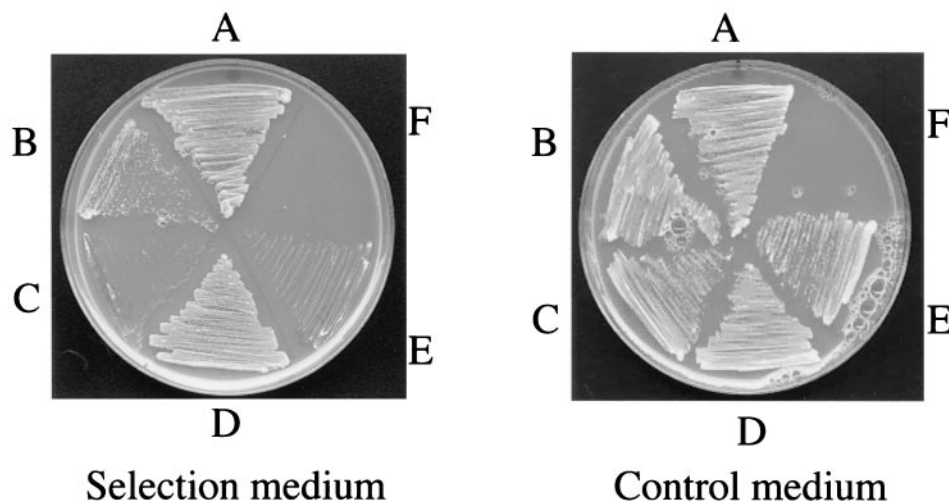


FIG. 8. Pf20-WD can interact with Spag6 *in vivo*. The open reading frame of TB-RBP and the cDNA encoding WD repeats of Pf20 were cloned in frame into the pBD-GAL4cam plasmid. The open reading frames of TB-RBP and Spag6 and the cDNA encoding the truncated TB-RBP₂₀₅ mutant were cloned in frame into the pAD-GAL4 plasmid. Pairs of BD and AD plasmids were cotransformed and streaked on SD plates lacking leucine, tryptophan, and histidine with growth indicating interaction. (A) BD-TB-RBP + AD-TB-RBP; (B) BD-TB-RBP + AD-TB-RBP₂₀₅; (C) BD-TB-RBP + AD-Spag6; (D) BD-Pf20-WD + AD-Spag6; (E) BD-Pf20-WD + AD-TB-RBP; (F) empty segment. These studies confirmed an interaction of Spag6 and the Pf20 WD repeats.

human testis (Fig. 3). A 1-kb transcript was detected in human testis that was not observed in the mouse. To characterize the two transcripts, Northern blot hybridization was performed with a 5' probe and a 3' probe. Only the 2.5-kb transcript in testis was detected with the 5' probe (Fig. 4), while the 3' probe detected both the 1.4- and 2.5-kb transcripts. A cDNA sequence previously deposited in GenBank (accession no. AK016618) encodes a transcript containing exons 12 to 19 and a 5' untranslated region in the intron preceding exon 12. Our findings coupled with the existence of an mRNA derived from transcription initiated in the intron in front of exon 12 suggest that there are two transcription start sites in the murine *Pf20* gene, one giving rise to an mRNA encompassing exons 1 to 19 and the other giving rise to an mRNA encompassing exons 12 to 19.

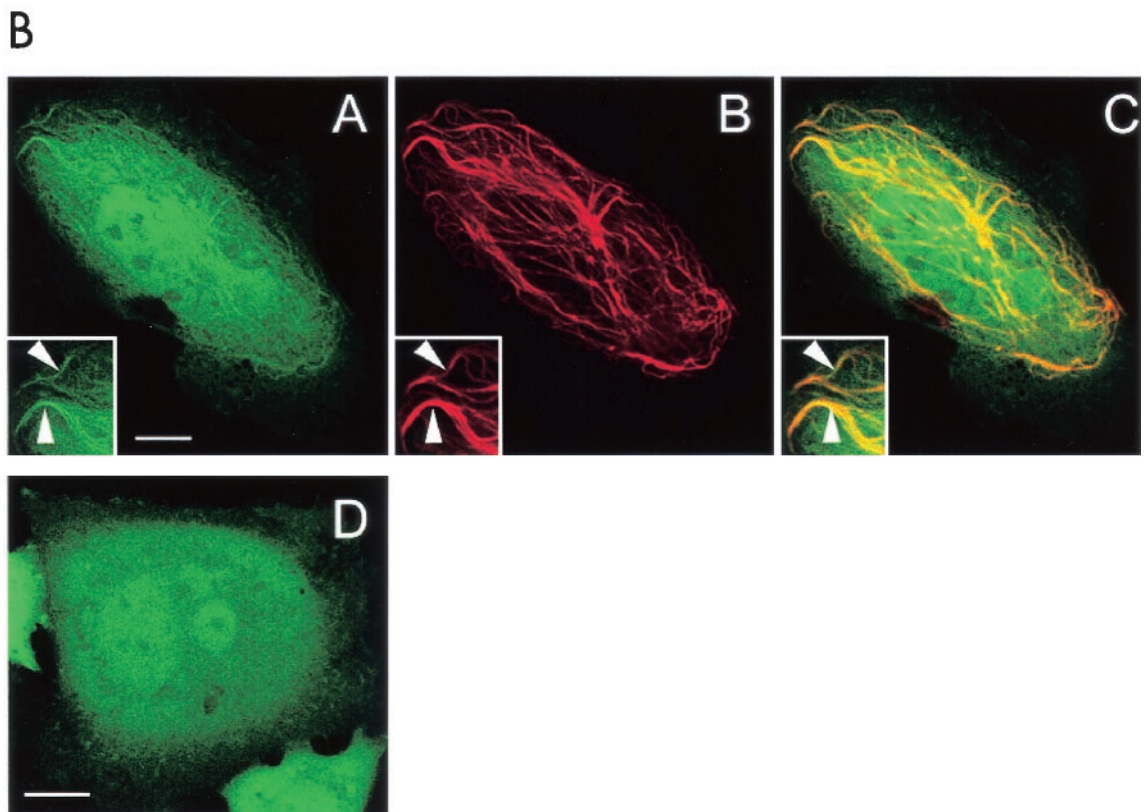
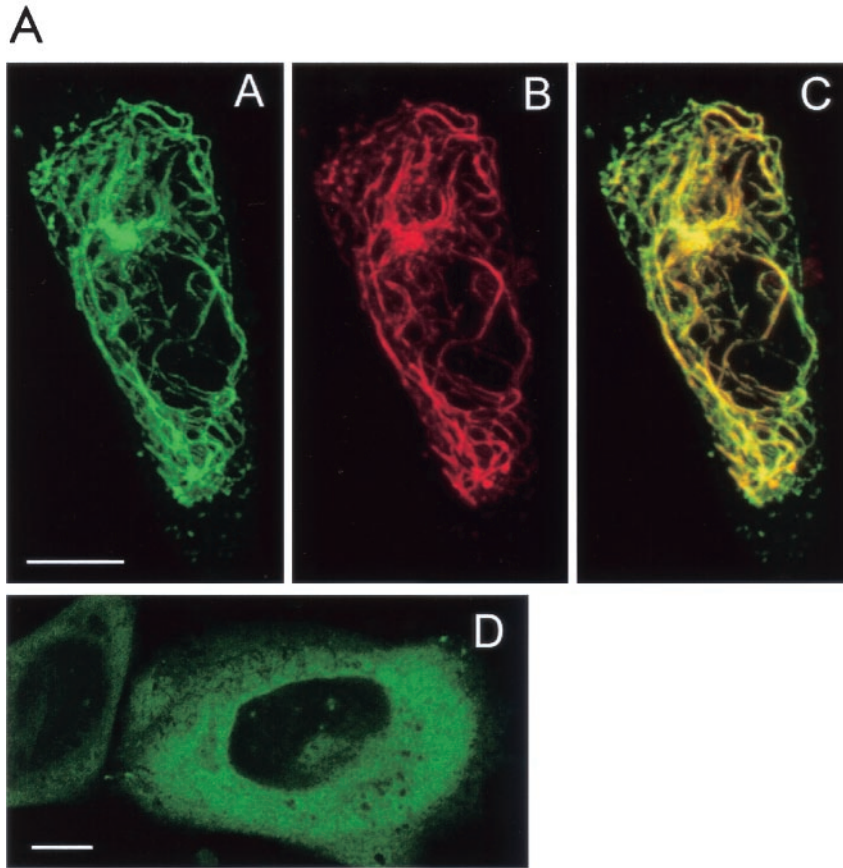
Mouse male germ cells expressed Pf20 (Fig. 5). The presence of Pf20 mRNA at the pachytene stage indicates that the *Pf20* gene is meiotically expressed, as is Spag6, another gene encoding an axonemal protein (9). Western blot analysis demonstrated the presence of a 71-kDa protein in extracts of mouse sperm and testis, consistent with the predicted size of the protein from the mouse cDNA sequence representing the 2.5-kb transcript (Fig. 6). The apparent absence of Pf20 mRNA and protein from other tissues does not necessarily mean that the gene is not expressed in those organs, as ciliated cells would have represented a small fraction of the tissue and low levels of mRNA or protein may have gone undetected. Because our antibody was generated against N-terminal sequences that would be excluded from the protein encoded by the 1.4-kb transcript, we cannot determine whether this transcript is indeed translated.

Localization of Pf20 in mouse sperm. Pf20 was detected along the tails of permeabilized mouse sperm by indirect immunofluorescence (Fig. 7A). Neutralization of the antiserum with the purified recombinant antigen inhibited the signal.

Some staining was seen in the acrosome, a common nonspecific reaction seen with many antibodies. Electron microscopic immunocytochemistry revealed a clustering of gold-labeled antibody in the axoneme core, with higher-magnification images indicating that Pf20 is located in the axoneme central apparatus (Fig. 7B), a position consistent with the known location of the *Chlamydomonas* protein. Our experiments, however, could not determine if mouse Pf20 is asymmetrically arranged along the central pair microtubules as it is in algae.

Pf20 interacts with Spag6, the mammalian orthologue of *Chlamydomonas* PF16. In preliminary studies in which we were seeking interacting partners for Pf20 by a yeast two-hybrid screen with the Pf20 WD repeats as bait and a mouse male germ cell library, we identified Spag6 as a potential partner in two of nine clones examined. In further exploring this interaction, we showed that BD-Pf20-WD interacts with AD-Spag6, providing additional evidence for Pf20-Spag6 interaction (Fig. 8). As a positive control for the yeast two-hybrid interaction, we utilized the well-established homodimerization of TB-RBP (2, 5, 37). TB-RBP weakly interacts with the TB-RBP₂₀₅ mutant as previously reported and provides an estimate of interaction strength for this experiment (37). However, TB-RBP does not interact with either Spag6 or Pf20-WD, which demonstrates that Pf20-WD specifically interacts with Spag6.

The 97-kDa Pf20-GFP fusion protein accumulated in the cytoplasm of transfected Chinese hamster ovary cells (Fig. 9). A Spag6-RFP construct decorated a subset of polymerized microtubules, consistent with our previous studies demonstrating that Spag6 associates with microtubules (29). When the Spag6-RFP and Pf20-GFP constructs were cotransfected into Chinese hamster ovary cells, the proteins were colocalized on microtubules (Fig. 9A, subpanels A, B, and C). A GFP fusion protein containing only the Pf20 WD repeats was localized to the cytoplasm (Fig. 9B, subpanel D) but also colocalized with Spag6-RFP on microtubules in cotransfected cells (Fig. 9B,



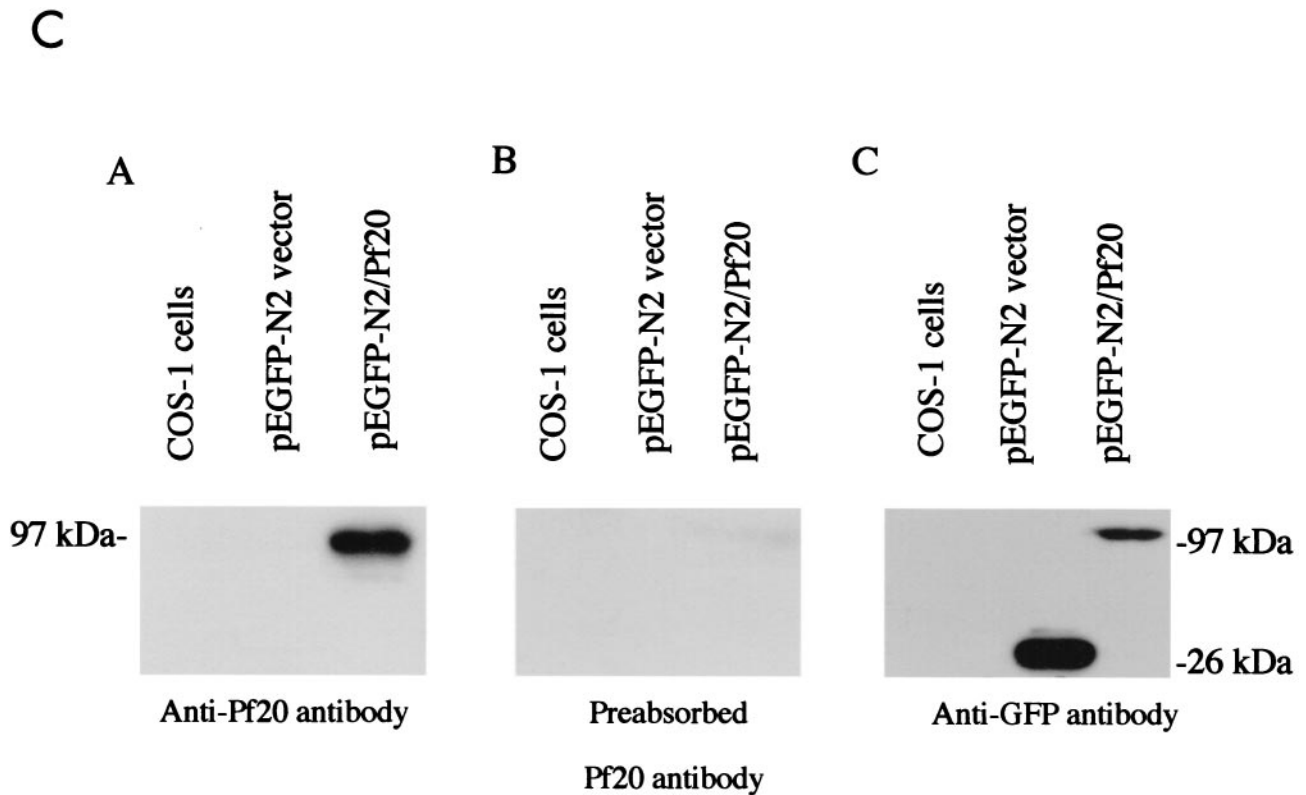


FIG. 9. Association of Pf20 with Spag6. (A) Spag6-RFP induces Pf20-GFP localization to microtubules in cotransfected CHO cells. Living CHO cells were cotransfected with Spag6-RFP and Pf20-GFP. In cells that were coexpressing both Spag6-RFP and Pf20-GFP, Spag6-RFP (subpanel B) was found to be exclusively colocalized with Pf20-GFP (subpanel A) in a subset of microtubules. The overlap is shown in subpanel C. In living CHO cells that were transfected with Pf20-GFP alone (subpanel D), Pf20-GFP was found dispersed in a cytoplasmic pattern and no Pf20-GFP labeled microtubules were observed in the transfected cells. All are confocal images. Images A, B, and C are projections of eight z-section series, obtained with simultaneous dual-color scanning (bars = 10 μ m). (B) A portion of Pf20 WD-GFP binds to Spag6-RFP-labeled microtubules in cotransfected CHO cells. (Subpanels A to C) Living CHO cells cotransfected with Spag6-RFP and Pf20 WD-GFP. In cells coexpressing both constructs, Pf20 WD-GFP (subpanel A) was found to colocalize to Spag6-RFP-labeled microtubules (subpanel B). Arrowheads in insets in subpanels A, B, and C show colocalization of Pf20 WD-GFP (subpanel A) and Spag6-RFP (subpanel B) in microtubules. Subpanel C is a merged image of subpanels A and B. Pf20 WD-GFP (subpanel D) is present in a cytoplasmic and nuclear pattern when expressed alone in CHO cells, and no Pf20 WD-GFP-labeled microtubules were found in the transfected cells. All are confocal images. Images A, B, and C are projections of eight z-section series, obtained with simultaneous dual-color scanning (bars = 10 μ m). (C) Western blot analysis of Pf20 in extracts of transfected COS-1 cells. COS-1 cells were transfected with mouse Pf20 cDNA (pEGFP/Pf20) or empty vector. (Subpanel A) Total extract of COS-1 cells showing expression of Pf20-GFP in cells transfected with Pf20-GFP cDNA but no expression in nontransfected COS-1 cells or cells transfected with the empty plasmid vector. (Subpanel B) The same as subpanel A, except that the antibody was blocked by the purified protein. Subpanel C shows that COS-1 cells transfected with pEGFP vector and pEGFP/Pf20 express the GFP.

subpanels A, B, and C). These observations suggest that the localization of Pf20 on the microtubules of axonemes is dependent upon and mediated by Spag6, probably through the Pf20 WD repeats.

Pf20 is markedly reduced in sperm collected from mice lacking Spag6. Mice deficient in Spag6 were recently created by gene targeting (28). Male mice lacking Spag6 are infertile due to a sperm motility defect that is associated with disorganization of the axoneme including loss of the central apparatus and associated structures (outer dense fibers and fibrous sheath) in the tail. Western blotting and immunofluorescence analysis of sperm from three different Spag6^{-/-} male mice revealed that Pf20 was markedly reduced whereas the major protein of the fibrous sheath, Akap82, also known as Akap4 (28), was present, albeit at a slightly reduced level, consistent with the ultrastructural disorganization of the fibrous sheath that was previously described for epididymal sperm from

Spag6-deficient mice (28) (Fig. 10 and 11). Pf20 mRNA was present in testis of Spag6-deficient mice at levels comparable to that in wild-type testis, indicating that the loss of Pf20 is not a consequence of altered gene expression. Moreover, some Pf20 was detectable in testis extracts. Thus, the Pf20 protein is evidently degraded in the absence of Spag6 prior to the time at which sperm reach the epididymis.

DISCUSSION

We describe here the cloning of cDNAs encoding human and mouse proteins that have high homology with *Chlamydomonas* PF20. Database searches using the predicted amino acid sequences of mouse and human PF20 placed the protein in the family of proteins that contain WD repeat domains. WD domains are made up of highly conserved repeating units usually ending with Trp-Asp (WD). They are found in all eu-

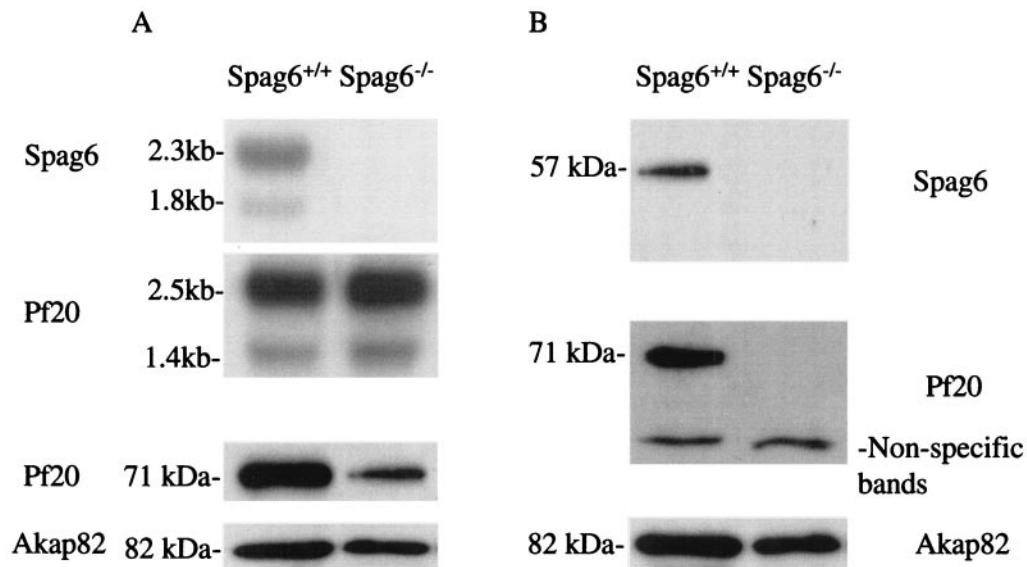


FIG. 10. Pf20 mRNA and protein expression in *Spag6*^{+/+} and *Spag6*^{-/-} mice. (A) (upper two panels) Northern blot analysis of testicular RNA for *Spag6* and Pf20; (lower panel) Western blot analysis for Pf20 and Akap82 in testicular extracts. (B) Western blot analysis of epididymal sperm from wild-type and *Spag6*-deficient mice for *Spag6*, Pf20, and Akap82.

karyotes but not in prokaryotes. The WD repeat motifs, first identified in the β subunit of G proteins (19), are believed to mediate protein-protein interactions (19) and regulate cellular functions, such as transmembrane signaling, cell division, cell fate determination, gene transcription, mRNA modification, ribosome biosynthesis, and vesicle fusion (12, 21, 22, 30, 38). An increasing number of axoneme proteins have been found to contain WD repeats, and evidence suggests that this feature is important for regulation of flagellar motility (22). *Chlamydomonas* PF20 is located in the bridge that connects the C1 and C2 central apparatus microtubules (32), indicating that PF20 is positioned to play a role in the assembly and/or stability of the entire central apparatus through interactions with another protein(s).

While this work was being prepared for publication, Pennarun et al. reported the cloning of the human PF20 cDNA (21). The nucleotide and amino acid sequences of the cDNA reported by these authors are identical to ours. These authors also detected four PF20 transcripts in human testis by using a combination of Northern blotting and reverse transcription-PCR. Two of these transcripts contained sequences encoding the C-terminal WD repeats, and two encoded N-terminal sequences that would lack the WD repeats. They concluded that the latter represented the 1.4-kb mRNA based on its hybridization with a probe representing the putative 3' untranslated region of the transcripts. This conclusion contrasts with our findings, which indicate that the smaller transcript encodes the C terminus containing the WD repeats. A mouse cDNA se-

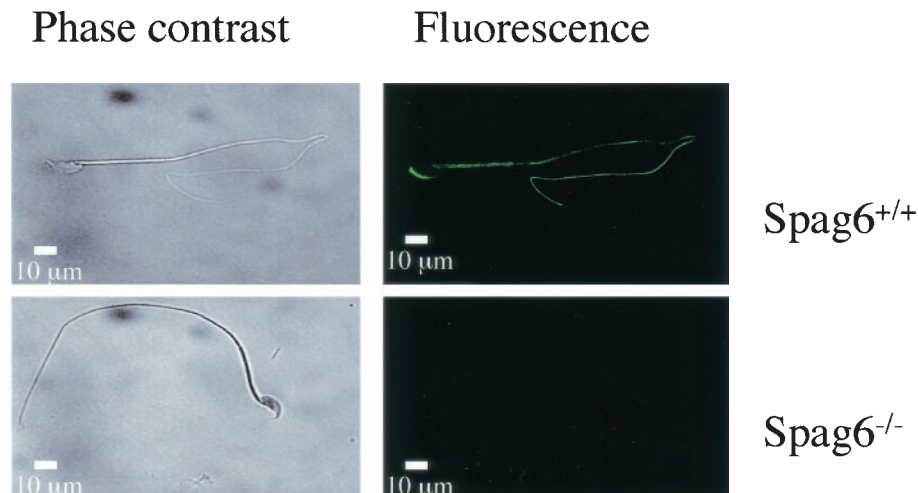


FIG. 11. Immunostaining of Pf20 in *Spag6*^{+/+} and *Spag6*^{-/-} sperm. Phase-contrast and corresponding immunofluorescence photomicrographs are shown of wild-type and *Spag6*-deficient Triton X-100-permeabilized sperm analyzed with anti-Pf20 antibody.

quence deposited by Carninci et al. (accession no. AK016618) contains an open reading frame encoding the C terminus of mouse Pf20 consistent with a transcript size of 1.4 kb. Consequently, the collective evidence indicates that the 1.4-kb transcript in the mouse is derived from an alternative transcriptional start site yielding an mRNA that encodes a protein containing the C terminus of Pf20. However, it must be recognized that we did not determine whether mouse transcripts exist corresponding to the short human variants reported by Pennarun et al. (21). The discrepancies between the findings in the human and mouse tissues may be explained by species differences. Consistent with this idea, Pennarun et al. (21) concluded that the human *PF20* gene is composed of 16 exons whereas our analysis based on data deposited in public databases of mouse genomic sequences indicates that the murine *Pf20* gene is comprised of 19 exons.

The high level of Pf20 expression in the testis, its low abundance or apparent absence from other tissues, and localization of Pf20 to the sperm tail are consistent with a role for Pf20 in sperm flagellar structure or function. Whether the 1.4-kb mRNA encodes a protein and whether it has functions related to or distinct from those of the protein encoded by the 2.5-kb transcript remain to be determined, but both proteins contain the WD repeats which presumably mediate protein-protein interactions.

One of the proteins which appears to associate directly or indirectly with Pf20 is Spag6, another axonemal protein that binds to microtubules. The evidence supporting this notion includes the colocalization of Spag6 and Pf20 in cotransfected cells, yeast two-hybrid studies demonstrating that the Pf20 WD repeats interact with Spag6, and the loss of Pf20 from sperm lacking Spag6. The interactions between Spag6 and Pf20 may maintain the structural integrity of the axoneme and account for the loss of the central apparatus in Spag6-null mice (28). In *Chlamydomonas*, two-dimensional electrophoresis analysis revealed that the flagella of *pf16* mutants lack three proteins having molecular masses of 57 kDa (probably PF16) and 128 and 32 kDa, but PF20, with an estimated molecular mass of 66.6 kDa, is evidently not one of the three missing polypeptides (6). Thus, the Spag6-Pf20 interaction that we have observed may be a feature of mammalian but not algal axonemes. It should be noted that the methods that we have employed to assess Pf20-Spag6 interaction cannot distinguish between direct binding and binding through the intermediation of a linker protein. This possibility may be difficult to exclude experimentally, particularly if the ability of Spag6 to interact with Pf20 is augmented by Spag6 binding to microtubules. Whether other WD repeat-containing proteins also associate in a similar fashion with Spag6 is a question of interest that requires further investigation.

In summary, we have cloned cDNAs encoding the mammalian orthologues of a *Chlamydomonas* WD repeat-containing protein, PF20, known to be important for axoneme assembly and function in algae. The mammalian and algal proteins are highly conserved. We have also obtained evidence that Pf20 interacts with another axoneme protein, the armadillo repeat-containing Spag6, which is important for axoneme motility and stability in *Chlamydomonas* (31, 32) and mice (28). If Pf20 and Spag6 are asymmetrically distributed along the central pair microtubules in mammalian axonemes as they are in *Chlamy-*

domonas, the interactions between these proteins identified in the present work provide a mechanism for communication between the two central pair microtubules.

ACKNOWLEDGMENTS

We thank Judy Wood for help in preparation of the manuscript. We express our gratitude to Paul A. Lefebvre (University of Minnesota) and Emer M. Smyth (University of Pennsylvania) for helpful comments during the course of this work.

These studies were supported by NIH grant R01-HD37416-02; R.S. was a Fogarty International Center Scholar supported by D43-TW/HD00671; J.B. was supported by T32-HD07305. The immunoelectron microscopy was performed in the Imaging Core of the University of Pennsylvania Diabetes Center, supported by DK19525.

REFERENCES

- Adams, G. M. W., B. Huang, G. Piperno, and D. J. L. Luck. 1981. Central-pair microtubular complex of *Chlamydomonas* flagella: polypeptide composition as revealed by analysis of mutants. *J. Cell Biol.* **91**:69–76.
- Aoki, K., R. Ishida, and M. Kasai. 1997. Isolation and characterization of a cDNA encoding a translin-like protein, TRAX. *FEBS Lett.* **401**:109–112.
- Barkalow, K., T. Hamasaki, and P. Satir. 1994. Regulation of 22S dynein by a 29-kD light chain. *J. Cell Biol.* **126**:727–735.
- Brokaw, C. J., and R. Kamiya. 1987. Bending patterns of *Chlamydomonas* flagella: IV. Mutants with defects in inner and outer dynein arms indicate differences in dynein arm function. *Cell Motil. Cytoskeleton.* **8**:68–75.
- Chennathukuzhi, V. M., Y. Kurihara, J. D. Bray, and N. B. Hecht. 2001. Trax (translin-associated factor X), a primarily cytoplasmic protein, inhibits the binding of TB-RBP (translin) to RNA. *J. Biol. Chem.* **276**:13256–13263.
- Dutcher, S. K., B. Huang, and D. J. L. Luck. 1984. Genetic dissection of the central pair microtubules of the flagella of *Chlamydomonas reinhardtii*. *J. Cell Biol.* **98**:229–236.
- Fox, L. A., and W. S. Sale. 1987. Direction of force generated by the inner row of dynein arms on flagellar microtubules. *J. Cell Biol.* **105**:1781–1787.
- Garcia-Higuera, I., J. Fenoglio, Y. Li, C. Lewis, M. P. Panchenko, O. Reiner, et al. 1996. Folding of proteins with WD-repeats: comparison of six members of the WD-repeat superfamily to the G protein beta subunit. *Biochemistry* **35**:13985–13994.
- Goldberg, R. B., R. Geremia, and W. R. Bruce. 1977. Histone synthesis and replacement during spermatogenesis in the mouse. *Differentiation* **7**:167–180.
- Hamasaki, T., K. Barkalow, J. Richmond, and P. Satir. 1991. CAMP-stimulated phosphorylation of an axonemal polypeptide that copurifies with the 22S dynein arm regulates microtubule translocation velocity and swimming speed in *Paramecium*. *Proc. Natl. Acad. Sci. USA* **88**:7918–7922.
- Huang, B., G. Piperno, and D. J. L. Luck. 1979. Paralyzed flagella mutants of *Chlamydomonas reinhardtii*. *J. Biol. Chem.* **254**:3091–3099.
- Huh, C. G., J. Aldrich, J. Mottahedeh, H. Kwon, C. Johnson, and R. Marsh. 1998. Cloning and characterization of *Physarum polycephalum* tectonins. Homologues of *Limulus* lectin L-6. *J. Biol. Chem.* **273**:6565–6574.
- Iouk, T. L., J. D. Aitchison, S. Maguire, and R. W. Wozniak. 2001. Rrb1p, a yeast nuclear WD-repeat protein involved in the regulation of ribosome biosynthesis. *Mol. Cell. Biol.* **21**:1260–1271.
- Kamiya, R., E. Kurimoto, and E. Muto. 1991. Two types of *Chlamydomonas* flagella mutants missing different components of inner-arm dynein. *J. Cell Biol.* **112**:441–447.
- King, S. M., and R. S. Patel-King. 1995. The Mr = 8,000 and 11,000 outer arm dynein light chains from *Chlamydomonas* flagella have cytoplasmic homologues. *J. Biol. Chem.* **270**:11445–11452.
- King, S. M., R. S. Patel-King, C. G. Wilkerson, and G. B. Witman. 1995. The 78,000 Mr intermediate chain of *Chlamydomonas* outer arm dynein is a microtubule-binding protein. *J. Cell Biol.* **131**:399–409.
- Kurimoto, E., and R. Kamiya. 1991. Microtubule sliding in flagellar axonemes of *Chlamydomonas* mutants missing inner- or outer-arm dynein; velocity measurements on new types of mutants by an improved method. *Cell Motil. Cytoskeleton.* **19**:275–281.
- Naranda, T., M. Kainuma, S. E. MacMillan, and J. W. Hershey. 1997. The 39-kilodalton subunit of eukaryotic translation initiation factor 3 is essential for the complex's integrity and for cell viability in *Saccharomyces cerevisiae*. *Mol. Cell. Biol.* **17**:145–153.
- Neer, E. J., C. J. Schmidt, R. Nambudripad, and T. F. Smith. 1994. The ancient regulatory-protein family of WD-repeat proteins. *Nature* **371**:297–300.
- Neilson, L. I., P. L. Schneider, P. G. Van Deerlin, M. Kiriakidou, D. A. Driscoll, M. C. Pellegrini, S. Millinder, K. K. Yamamoto, C. K. French, and J. F. Strauss III. 1999. cDNA cloning and characterization of a human sperm antigen (SPAG6) with homology to the product of the *Chlamydomonas* PF16 locus. *Genomics* **60**:272–280.

21. Pennarun, G., A.-M. Bridoux, E. Escudier, F. Dastot-Le Moal, V. Cacheux, S. Amsellem, and B. Duriez. 2002. Isolation and expression of the human hPF20 gene orthologous to *Chlamydomonas* Pf20. *Am. J. Respir. Cell Mol. Biol.* **26**:362–370.
22. Perrone, C. A., P. Yang, E. O'Toole, W. S. Sale, and M. E. Porter. 1998. The *Chlamydomonas* IDA7 locus encodes a 140-kDa dynein intermediate chain required to assemble the I1 inner arm complex. *Mol. Biol. Cell* **9**:3351–3365.
23. Piperno, G., B. Huang, and D. J. L. Luck. 1977. Two-dimensional analysis of flagellar proteins from wild-type and paralyzed mutants of *Chlamydomonas reinhardtii*. *Proc. Natl. Acad. Sci. USA* **74**:1600–1604.
24. Piperno, G., K. Mead, M. LeDizet, and A. Moscatelli. 1994. Mutations in the “dynein regulatory complex” alter the ATP-insensitive binding sites for inner arm dyneins in *Chlamydomonas* axonemes. *J. Cell Biol.* **125**:1109–1117.
25. Randal, J., T. Cavalier-Smith, A. McVittie, J. Warr, and J. Hopkins. 1967. Developmental and control processes in the basal bodies and flagella of *Chlamydomonas reinhardtii*. *Dev. Biol.* **1**(Suppl.):43–83.
26. Ringo, D. 1967. Flagellar motion and fine structure of the flagellar apparatus in *Chlamydomonas*. *J. Cell Biol.* **33**:543–571.
27. Sale, W. S., and P. Satir. 1977. The direction of active sliding of microtubules in *Tetrahymena* cilia. *Proc. Natl. Acad. Sci. USA* **74**:2045–2049.
28. Sapiro, R., I. Kostetskii, P. Olds-Clarke, G. L. Gerton, G. L. Radice, and J. F. Strauss III. 2002. Male infertility, impaired sperm motility, and hydrocephalus in mice deficient in sperm-associated antigen 6. *Mol. Cell. Biol.* **22**:6298–6305.
29. Sapiro, R., L. M. Tarantino, F. Velazquez, M. Kiriakidou, N. B. Hecht, M. Bucan, and J. F. Strauss III. 2000. Sperm antigen 6 is the murine homologue of the *Chlamydomonas reinhardtii* central apparatus protein encoded by the PF16 locus. *Biol. Reprod.* **62**:511–518.
30. Shugrue, C. A., E. R. Kolen, H. Peters, A. Czernik, C. Kaiser, L. Matoveik, A. L. Hubbard, and F. Gorelick. 1999. Identification of the putative mammalian orthologue of Sec31P, a component of the COPII coat. *J. Cell Sci.* **112**:4547–4556.
31. Smith, E. F., and P. A. Lefebvre. 1997. The role of central apparatus components in flagellar motility and microtubule assembly. *Cell Motil. Cytoskeleton.* **38**:1–8.
32. Smith, E. F., and P. A. Lefebvre. 1997. PF20 gene product contains WD repeats and localizes to the intermicrotubule bridges in *Chlamydomonas* flagella. *Mol. Biol. Cell* **8**:455–467.
33. Tanaka, Y., Z. Zhang, and N. Hirokawa. 1995. Identification and molecular evolution of new dynein-like protein sequences in rat brain. *J. Cell Sci.* **108**:1883–1893.
34. Van Etten, W. J., R. G. Steen, H. Nguyen, A. B. Castle, D. K. Slonim, B. Ge, C. Nusbaum, G. D. Schuler, E. S. Lander, and T. J. Hudson. 1999. Radiation hybrid map of the mouse genome. *Nat. Genet.* **22**:384–387.
35. Warner, F. D., and P. Satir. 1974. The substructure of ciliary microtubules. *J. Cell Sci.* **12**:313–326.
36. Williams, B. D., M. A. Velleca, A. M. Curry, and J. L. Rosenbaum. 1989. Cloning and sequence analysis of the *Chlamydomonas* gene coding for radial spoke protein 3: flagellar mutation *pf-14* is an ochre allele. *J. Cell Biol.* **109**:235–245.
37. Wu, X. Q., L. Xu, and N. B. Hecht. 1998. Dimerization of the testis brain RNA-binding protein (translin) is mediated through its C-terminus and is required for DNA- and RNA-binding. *Nucleic Acids Res.* **26**:1675–1680.
38. Zhu, W., E. K. Chan, J. Li, P. Hemmerich, and E. M. Tan. 2001. Transcription activating property of autoantigen SG2NA and modulating effect of WD-40 repeats. *Exp. Cell Res.* **269**:312–321.